JCTC Journal of Chemical Theory and Computation

Article

pubs.acs.org/JCTC

Bulk Properties of Transition Metals: A Challenge for the Design of Universal Density Functionals

Patanachai Janthon,[†,‡,§] Sijie (Andy) Luo,[∥] Sergey M. Kozlov,[†] Francesc Viñes,[†] Jumras Limtrakul,[‡,§] Donald G. Truhlar,[∥] and Francesc Illas*[,†]

[†]Departament de Química Física & Institut de Química Teòrica i Computacional (IQTCUB), Universitat de Barcelona, c/Martí i Franquès 1, 08028, Barcelona, Spain

[‡]Department of Chemistry and NANOTEC Center for Nanoscale Materials Design for Green Nanotechnology, Kasetsart University, Bangkok 10900, Thailand

[§]PTT Group Frontier Research Center, PTT Public Company Limited, 555 Vibhavadi Rangsit Road, Chatuchak, Bangkok 10900, Thailand

[∥]Department of Chemistry, Chemical Theory Center, and Supercomputing Institute, University of Minnesota, Minneapolis, Minnesota 55455-0431, United States

Supporting Information

ABSTRACT: Systematic evaluation of the accuracy of exchange-correlation functionals is essential to guide scientists in their choice of an optimal method for a given problem when using density functional theory. In this work, accuracy of one Generalized Gradient Approximation (GGA) functional, three meta-GGA functionals, one Nonseparable Gradient Approximation (NGA) functional, one meta-NGA, and three hybrid GGA functionals was evaluated for calculations of the closest interatomic distances, cohesive energies, and bulk moduli of all 3d, 4d, and 5d bulk transition metals that have face centered cubic (fcc), hexagonal closed packed (hcp), or body centered cubic (bcc) structures (a total of 27 cases). Our results show that including the extra elements of kinetic energy density and Hartree−Fock exchange energy density into gradient approximation density functionals does not usually improve them. Nevertheless, the accuracies of the Tao−Perdew−Staroverov−Scuseria (TPSS) and M06-L meta-GGAs and the MN12-L meta-NGA approach the accuracy of the Perdew−Burke−Ernzerhof (PBE) GGA, so usage of these functionals may be advisable for systems containing both solid-state transition metals and molecular species. The N12 NGA functional is also shown to be almost as accurate as PBE for bulk transition metals, and thus it could be a good choice for studies of catalysis given its proven good performance for molecular species.

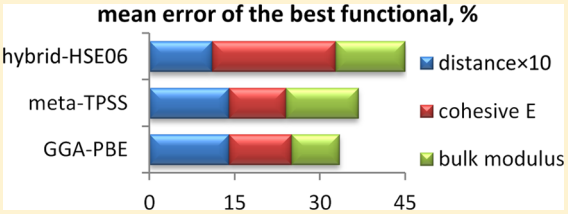

1. INTRODUCTION

Kohn−Sham Density Functional Theory (KS-DFT) has become a workhorse for treating complex problems in both the gaseous and condensed phases. The accuracy of KS-DFT rests entirely on the accuracy of one's approximation to the exchange-correlation (xc) functional. Functional development has considered a wide range of application targets. In particular, there are numerous validation studies for atoms and molecules, many more than for condensed-phase quantum chemistry and solid-state physics. A particularly important area that still needs further study in its own right, in addition to its importance for studying heterogeneous catalysis and electrochemistry,[1] is the accuracy of available xc functionals for transition metal solids.

One route to improving xc functionals is to add more elements, which takes one to a higher rung on the Jacob's ladder[2] of xc functionals. The first rung is the Local Spin Density Approximation (LSDA), where the xc functional depends on only local spin densities. Including dependences not only on spin densities but also on their gradients yields gradient approximations, such as the Generalized Gradient Approximation[3,4] (GGA) or Nonseparable Gradient Approximation[5] (NGA), which constitute the second rung; further addition of kinetic energy density leads to meta functionals, such as meta-GGAs and meta-NGAs, which form the third rung, and, finally, including Hartree−Fock (HF) exchange leads to hybrid functionals, in particular hybrid gradient approximations and hybrid meta approximations, which form the fourth rung. Through the third rung, the exchange-correlation energy density depends only on local variables, but hybrid functionals are nonlocal.

One tentative conclusion about xc functionals that has been advanced is that adding elements from the third and fourth rungs has not (with some exceptions) led to better performance for molecules containing metals,[6,7] and various studies have been carried out with gradient approximations that provide further experience related to this issue.[7−9] Furthermore, although hybrid functionals are justifiably the most popular

Received: June 20, 2014
Published: August 6, 2014

   dx.doi.org/10.1021/ct500532v | J. Chem. Theory Comput. 2014, 10, 3832−3839

kind of functionals in molecular chemistry[10] (because of their good performance), for extended systems they have increased computational demands as compared to local functionals due to the long range of the exchange in real space programs and to the requirement for dense Brillouin zone sampling in plane wave programs.[11] Hybrid functionals also have the disadvantage of bringing in HF static correlation error, which is important for many molecular and solid-state transition metal compounds.[6−9,12,13] In fact, when one tries to estimate the optimal percentage of HF exchange in a hybrid functional suitable for transition metal solids, the resulting fraction is close to zero,[14,15] leading to the conclusion that the inclusion of HF exchange is detrimental for the accuracy of xc functionals for solid transition metals. The problems with Hartree−Fock exchange for metals are in fact well-known in that Hartree−Fock exchange for free electrons (which constitute the zeroth-order model of a metal) leads to an unphysical density of states such that there is a singularity in the electron group velocity at the Fermi level, although this defect is eliminated if the Hartree−Fock exchange is screened by correlation effects.[16]

As a result of the above kinds of issues with including Hartree−Fock exchange—cost, performance, and an incorrect treatment of the density of states—local functionals have remained the most popular choice for solid-state transition metal investigations even though hybrid functionals by construction reduce self-interaction error. A similar situation pertains even when the choice of xc functionals is restricted to local ones, where, although meta functional also has the potential to reduce self-interaction error,[17] gradient approximations have been preferred to meta functionals partly for the greater simplicity of popular GGAs, but also because meta functionals have not always seemed to significantly improve the accuracy. However, this situation seems unsatisfactory because both hybrid functionals and meta functionals have better performance than GGAs on molecules composed of atoms lighter than the transition metals.[18−21] Thus, there is a strong interest in certain fields, such as heterogeneous catalysis, nanotechnology, and materials chemistry, to use meta or hybrid functionals because these research lines often deal with the interaction between transition metal surfaces and light main-group compounds. Meta and hybrid functionals also yield more accurate band gaps,[15,22,25] which may be important for metal-oxide systems that are ubiquitous as supports in catalysis, photocatalysis, and nanotechnology. In light of these practical considerations, there is a need for a more systematic investigation of the accuracy of meta and hybrid functionals for various properties of transition metal solids.

In this article, we assess the accuracy of several meta and hybrid functionals for bulk transition metals. Namely, we consider shortest interatomic distances, δ, cohesive energies, E_{coh}, and bulk moduli, B_0, of all 27 bulk transition metals that have face centered cubic (fcc), hexagonal closed packed (hcp), or body centered cubic (bcc) structures. We present new results for the following functionals: GGA: SOGGA11;[26] NGA: N12;[5] meta-GGAs: Tao−Perdew−Staroverov−Scuseria (TPSS),[27] revised Tao−Perdew−Staroverov−Scuseria (revTPSS),[28] and meta M06-L;[29] meta-NGA: MN12-L;[30] hybrid gradient approximations with unscreened Hartree−Fock exchange: Perdew−Burke−Ernzerhof (PBE0),[31,32] and Lee−Yang−Parr B3LYP;[32] and hybrid gradient approximation with screened Hartree−Fock exchange: Heyd−Scuseria−Ernzerhof (HSE06).[33]

We compare the new results obtained here to the results obtained previously[34] with PBE, a GGA functional that performed best in a previous study of two LSDA functionals [the Perdew−Zunger functional (PZ81)[35] based on Ceperley−Alder (CA) numerical results[36] and the Vosko−Wilk−Nusair functional (VWN, usually denoted also as VWN5)][37] and four gradient approximations [PBE,[38] PBEsol,[39] RPBE,[40] and PW91[41]]. Note that the performance of the PW91 GGA was found to be close to that of PBE.

2. COMPUTATIONAL DETAILS

The computational procedures were kept as close as possible to those used in a previous work by Janthon et al.[34] Calculations were performed using a locally modified version of the Vienna Ab Initio Simulation Package (VASP).[42] The atomic cores were described by the Projector Augmented Wave (PAW) method,[43] using the potentials recommended in the documentation (see Table S1 in the Supporting Information for full specification) which take account of kinetic energy density dependencies when present. An optimized Monkhorst−Pack[44] **k**-points grid of $7 \times 7 \times 7$ was used in all bulk calculations, which was found to be sufficient for accurate total energy calculations with the smallest unit cell. A kinetic energy cutoff of 415 eV for the plane-wave basis set was employed throughout, guaranteeing variations of total energy below 1 meV with respect to more complete basis sets.

Scalar relativistic effects in the core region are included in the PAW potentials. Previous calculations have shown that relativistic effects on the valence electrons of heavy transition metals lead to negligible deviations from this standard PAW approximation, i.e., interatomic distance changes in the 0.002−0.005 Å range and differences in bulk moduli of 3−5 GPa.[45]

The electronic structure calculations were not spin polarized, with the exception of the calculations on the ferromagnetic Fe, Ni, and Co bulk systems and on isolated metal atoms. Although it is a digression, we note in passing that some of the calculated magnetic moments agree nicely with experimental values. For instance, the PBE values of 2.21, 1.55, and 0.59 μ_B agree well with experimental values of 2.2, 1.7, and 0.6 μ_B for Fe, Co, and Ni, respectively.[46] Values predicted by TPSS are very close to the PBE ones with differences smaller than 0.02 μ_B, whereas HSE06 overestimates the magnetic moments with predicted values of 2.89, 1.85, and 0.82 μ_B for Fe, Co, and Ni, respectively. Note also that, even though a nearly degenerate antiferromagnetic solution for the bulk structure of Cr with a magnetic moment of of 0.92 μ_B has been reported from calculations at the PW91 level,[47] the present calculations for Cr correspond to a nonmagnetic solution.

Optimizations were performed using the tetrahedron smearing method of Blöchl et al.[48] with an energy width of 0.2 eV to speed up convergence with the final energies extrapolated to zero smearing. In bulk calculations, ionic positions and cell volumes were optimized using the conjugate gradient algorithm until pressures and total energies were converged within 0.01 GPa and 10 meV, respectively.

Calculated cohesive energies are sensitive to the treatment adopted for calculating the energies of the atoms. The isolated atoms were placed in a large unit cell with a broken symmetry of $9 \times 10 \times 11$ Å dimensions to ensure proper occupancy of orbitals. When needed, orbital occupancy was imposed to match that of the isolated atom; further details concerning atomic configuration and energies are found in a previous article.[34] The large unit cell allows one to sufficiently suppress

Table 1. Calculated and Experimental Shortest Interatomic Distances (δ, in Å) for Bulk Transition Metals

		GGA		NGA	meta-GGA			meta-NGA	hybrid				
	CS	PBE	SOGGA11	N12	TPSS	revTPSS	M06-L	MN12-L	PBE0	HSE06	B3LYP	exptl.	exptl. corr.[a]
Sc	hcp	3.214	3.066	3.194	3.198	3.192	3.149	3.013	3.238	3.252	3.230	3.254	3.244
Ti	hcp	2.884	2.806	2.864	2.862	2.855	2.859	2.850	2.862	2.865	2.883	2.897	2.889
V	bcc	2.577	2.561	2.582	2.559	2.554	2.581	2.559	2.548	2.548	2.573	2.613	2.606
Cr	bcc	2.459	2.479	2.467	2.442	2.435	2.457	2.428	2.429	2.428	2.457	2.498	2.485
Fe	bcc	2.453	2.498	2.457	2.431	2.424	2.484	2.598	2.502	2.522	2.517	2.460	2.450
Co	hcp	2.470	2.496	2.438	2.444	2.438	2.472	2.489	2.452	2.482	2.498	2.497	2.488
Ni	fcc	2.489	2.506	2.455	2.453	2.443	2.419	2.370	2.471	2.480	2.510	2.493	2.484
Cu	fcc	2.567	2.502	2.551	2.517	2.499	2.476	2.485	2.563	2.564	2.606	2.556	2.544
Zn	hcp	2.644	2.558	2.658	2.522	2.465	2.490	2.552	2.638	2.640	2.781	2.665	2.645
Y	hcp	3.543	3.419	3.511	3.522	3.518	3.562	3.615	3.554	3.559	3.565	3.556	3.548
Zr	hcp	3.197	3.144	3.166	3.179	3.171	3.218	3.195	3.187	3.185	3.213	3.179	3.174
Nb	bcc	2.873	2.882	2.871	2.862	2.852	2.888	2.871	2.860	2.857	2.888	2.859	2.854
Mo	bcc	2.749	2.716	2.692	2.734	2.729	2.748	2.726	2.724	2.721	2.755	2.725	2.721
Tc	hcp	2.722	2.707	2.685	2.700	2.689	2.706	2.689	2.679	2.677	2.717	2.710	2.705
Ru	hcp	2.658	2.643	2.627	2.637	2.624	2.649	2.623	2.608	2.610	2.649	2.650	2.642
Rh	fcc	2.717	2.695	2.683	2.689	2.674	2.702	2.676	2.674	2.672	2.723	2.539	2.532
Pd	fcc	2.794	2.756	2.766	2.761	2.742	2.794	2.755	2.768	2.765	2.827	2.753	2.745
Ag	fcc	2.941	2.861	2.901	2.890	2.867	2.940	2.899	2.924	2.925	2.992	2.889	2.877
Cd	hcp	2.990	2.941	3.018	2.920	2.880	2.883	3.002	2.964	2.971	3.139	2.979	2.959
Hf	hcp	3.139	3.067	3.110	3.114	3.100	3.151	3.099	3.123	3.151	3.148	3.131	3.126
Ta	bcc	2.875	2.875	2.854	2.857	2.844	2.886	2.839	2.864	2.861	2.886	2.860	2.856
W	bcc	2.751	2.761	2.746	2.736	2.724	2.744	2.718	2.725	2.724	2.761	2.741	2.738
Re	hcp	2.755	2.756	2.723	2.742	2.730	2.742	2.724	2.721	2.720	2.759	2.567	2.562
Os	hcp	2.694	2.700	2.673	2.685	2.673	2.688	2.656	2.660	2.661	2.698	2.675	2.671
Ir	fcc	2.741	2.747	2.712	2.727	2.710	2.733	2.705	2.712	2.711	2.759	2.715	2.710
Pt	fcc	2.811	2.809	2.780	2.789	2.769	2.806	2.771	2.778	2.777	2.835	2.772	2.766
Au	fcc	2.950	2.921	2.912	2.912	2.888	2.945	2.913	2.922	2.919	2.992	2.879	2.870

[a]ZPE and finite temperature corrections to experimental values adapted from Lejaeghere et al.[52]

spurious interactions between periodic images (<1 meV). Calculations of isolated atoms were carried out at the Γ point in reciprocal space.

For the purpose of comparing calculations on bulk metals to calculations on metal dimers and clusters, it is more physical to consider shortest interatomic distances in a crystal than to consider lattice constants. For fcc and bcc structures, the shortest interatomic distances, δ, within a crystal cell may be calculated from the lattice parameter a. For the fcc structures δ equals $a/\sqrt{2}$, while for bcc it equals $\sqrt{3}a/2$. In the case of hcp, δ depends on lattice parameters a and c, and δ may equal a or $(c^2/4 + a^2/3)$ depending on the c/a ratio.

Cohesive energies, E_{coh}, were expressed as an energy difference per atom as follows:

$$E_{coh} = E_{at} - \frac{E_{bulk}}{N}$$

where E_{at} is the energy of the isolated metal atom in a vacuum and E_{bulk} is the energy of the bulk unit cell containing N atoms. With this definition, the larger the positive values of cohesive energies, the stronger is the chemical bonding within the solid.

The bulk modulus, B_0, is defined as

$$B_0 = -V_0\left(\frac{\partial P}{\partial V}\right)_{T,Vo}$$

where V is the volume of the solid, P is an external pressure, and the negative sign is used because the volume decreases when a positive external pressure is applied. Bulk modulus is obtained as the slope of linear regression of P versus V using the volumes at the equilibrium geometry and at geometries with ±0.05 and ±0.10 Å variations of the lattice constants. A more accurate procedure would be the adjustment of energy points to a Murnaghan equation of state.[49] Bulk moduli obtained at the PBE level with a similar calculation setup but through the adjustment to the Murnaghan equation are ∼5 GPa lower than those calculated here.[11]

In the present work, we consider the 27 transition metals that exhibit close-packed structures, which may display fcc, hcp, or that exhibit a bcc structure. We specifically exclude La and solid Hg, which have hexagonal and rhombohedral unit cells, respectively, and Mn, which has a cubic unit cell containing 58 atoms, although it is similar to a bcc structure. The reason for these exclusions is that preliminary work showed that metals exhibiting these structures can exhibit different trends than the typical metals, and specialized consideration is required to do them justice.

In the following, as in the previous work,[34] in addition to cohesive energy and bulk modulus, the shortest interatomic distance within a crystal cell, δ, will be compared to the experimental values. We present results for individual metals, and to more clearly see some trends, we also present mean errors, in particular mean signed error (MSE), mean absolute error (MAE), and mean absolute percentage error (MAPE).

3. COMPARISON BETWEEN EXPERIMENTAL AND THEORETICAL RESULTS

To compare calculated results to the available experimental data in a reasonable fashion, we must take account of experimental variability and the differences between the measurements and

Table 2. Calculated and Experimental Cohesive Energies (E_{coh}, in eV/atom) of Bulk Transition Metals

		GGA		NGA	meta-GGA			meta-NGA	hybrid				
	CS	PBE	SOGGA11	N12	TPSS	revTPSS	M06-L	MN12-L	PBE0	HSE06	B3LYP	exptl.	exptl. corr.[a]
Sc	hcp	4.12	3.63	4.53	4.21	4.28	5.77	5.32	3.42	3.52	2.76	3.90	3.93
Ti	hcp	5.45	5.37	5.78	5.47	5.52	6.40	6.85	4.00	4.08	3.35	4.84	4.88
V	bcc	6.03	5.12	5.77	5.73	5.94	6.30	5.75	3.40	3.48	3.25	5.30	5.34
Cr	bcc	4.00	4.37	4.21	4.21	4.44	4.55	4.33	1.54	1.57	1.57	4.09	4.15
Fe	bcc	4.87	4.96	4.65	5.23	5.48	5.39	5.13	3.22	3.29	2.81	4.28	4.32
Co	hcp	5.27	4.28	5.32	6.21	6.51	5.66	4.54	3.24	3.31	2.86	4.43	4.47
Ni	fcc	4.87	4.11	4.96	5.40	5.24	5.75	6.15	3.19	3.26	2.85	4.44	4.48
Cu	fcc	3.48	3.32	3.36	3.73	4.06	4.39	4.42	3.01	3.06	2.54	3.48	3.51
Zn	hcp	1.12	0.86	1.14	1.34	1.59	1.67	1.58	1.12	1.17	0.44	1.35	1.38
Y	hcp	4.13	4.56	4.59	4.23	4.38	4.96	5.78	3.74	3.85	3.00	4.39	4.42
Zr	hcp	6.16	7.43	6.73	6.30	6.50	6.75	5.15	5.60	5.70	4.69	6.29	6.32
Nb	bcc	6.98	7.86	7.23	7.20	7.42	8.02	7.40	5.96	6.12	5.59	7.44	7.47
Mo	bcc	6.21	6.95	6.89	6.59	6.91	6.90	6.82	5.10	5.19	4.82	6.80	6.84
Tc	hcp	6.85	8.52	7.34	7.18	7.58	7.15	7.04	5.41	5.54	4.90	7.13	7.17
Ru	hcp	6.67	8.00	7.21	7.10	7.52	6.76	6.79	5.06	5.21	4.56	6.74	6.80
Rh	fcc	5.62	7.00	6.00	6.22	6.61	6.12	6.33	4.39	4.54	3.92	5.72	5.76
Pd	fcc	3.71	4.54	3.55	4.01	4.40	4.24	4.70	2.85	2.96	2.43	3.90	3.93
Ag	fcc	2.49	3.20	2.49	2.73	3.04	3.28	3.60	2.28	2.35	1.87	2.94	2.96
Cd	hcp	0.73	1.72	0.76	0.96	1.21	1.37	1.06	0.78	0.85	0.18	1.16	1.18
Hf	hcp	6.40	7.61	6.84	6.53	6.78	7.32	5.78	6.04	6.12	5.02	6.42	6.44
Ta	bcc	8.27	8.45	8.26	8.51	8.84	8.99	7.58	7.63	7.74	6.58	8.09	8.11
W	bcc	9.07	9.16	9.02	8.81	9.19	9.86	8.43	7.76	7.79	7.29	8.79	8.83
Re	hcp	7.82	7.97	7.89	8.25	8.68	7.97	9.45	6.75	6.85	5.89	8.02	8.06
Os	hcp	8.29	8.72	7.84	8.46	8.80	8.32	9.46	7.20	7.34	6.24	8.17	8.22
Ir	fcc	7.32	8.31	7.74	7.71	8.21	7.03	7.35	6.19	6.36	5.28	6.92	6.96
Pt	fcc	5.50	6.58	5.71	5.79	6.25	5.97	6.17	4.69	4.83	3.99	5.85	5.87
Au	fcc	2.99	3.86	3.03	3.28	3.62	3.61	3.79	2.80	2.88	2.23	3.81	3.83

[a]ZPE and finite temperature corrections to experimental values adapted from Lejaeghere et al.[52]

the calculations. First of all, significant differences can be found between experimental values reported for cohesive energies and bulk moduli in different sources, and on average, different entries in the Crystallographic Open Database[50] yield the shortest interatomic distances with variations of ∼0.05 Å. Among many entries in the database, we selected the most recent ones, as was done previously.[34] For cohesive energies and bulk moduli, we picked experimental values from the handbook by Young.[51] However, in a recent study by Lejaeghere et al.[52] assessing the performance of the PBE functional for almost all elemental solids in the periodic table, alternative sets of experimental values are used, mostly from Kittel or Villars and Daams.[53,54] See Tables S2−S4 in the Supporting Information for more details. With some exceptions, the experimental values used in the present work compare nicely to the values used in Lejaeghere et al., with median discrepancies for δ, E_{coh}, and B_0 being 0.004 Å, 0.06 eV, and 5 GPa, respectively. If we used the same set of experimental values as in ref 52, the reported MAPE would change by less than 0.5% for δ, 0.25% for E_{coh}, and 2% for B_0, and such changes have a negligible effect on our conclusions.

The second type of complication comes from the fact that experiments are typically performed at room temperature, whereas the calculations reported here reflect the internal energies at minima of potential energy surfaces. Results measured at room temperature differ from the calculated values mainly by inclusion of zero-point phonon energy and thermal phonon energy. Rather than account for these effects in each computation, reverse corrections are applied to the experimental values. Here, we apply the same corrections as in Lejaeghere et al.,[52] which decrease δ by 0.003−0.022 Å, increase E_{coh} by 0.01−0.06 eV, and increase B_0 by 1−17 GPa. In general, these corrections move experimental values closer to calculated ones, typically decreasing average MAPEs by 0.04%, 0.2%, and 2% for δ, E_{coh}, and B_0, respectively. For a clearer comparison with other studies, we list both corrected and uncorrected experimental values, but only corrected ones were used to calculate errors and draw conclusions.

4. RESULTS AND DISCUSSION

4.1. Interatomic Distances. In most of the cases studied here, the accuracy of KS-DFT for lattice constants is rather high. Table 1 shows ∼1% discrepancies between the calculated and the experimental data. One can compare the present results with previous computational studies carried out for a reduced set of metals. For instance, the present PBE results nicely correlate with previous calculations on Cu, Rh, Pd, and Ag fcc metals, with deviations below 0.01 Å.[11] Another suitable comparison with a previous study with over a dozen fcc and bcc transition metals revealed lattice parameter deviations of ∼0.03 Å for the PBE functional and below 0.02 Å for the TPSS functional,[55] corroborating the precision of the present calculations. Surprisingly, the most accurate xc functionals for interatomic distances are HSE06 and PBE0, which both slightly overestimate δ on average. Nevertheless, with the exception of HSE06 for Sc, all considered functionals underestimate interatomic distances of the lightest transition metals, Sc, Ti, V, and Cr. The present calculations reveal a nice match of HSE06 for Cr interatomic distances, whereas—for reasons that we do not understand—a previous study showed a considerable

Table 3. Calculated and Experimental Bulk Moduli (B_0, in GPa) of Bulk Transition Metals[a]

		GGA	meta-GGA			meta-NGA	hybrid				
	CS	PBE	TPSS	revTPSS	M06-L	MN12-L	PBE0	HSE06	B3LYP	exptl.	exptl. corr.[a]
Sc	hcp	55.0	59.4	57.9	71.6	82.5	57.2	56.2	51.4	54.6	55.6
Ti	hcp	113.5	119.1	122.6	129.4	125.4	132.4	125.2	120.0	106.0	108.3
V	bcc	183.1	198.9	212.0	193.3	199.1	225.9	214.9	199.1	155.0	158.9
Cr	bcc	261.2	274.4	293.3	268.6	298.4	290.7	291.8	271.8	160.0	174.5
Fe	bcc	195.3	218.5	232.8	169.8	77.2	165.1	176.7	151.1	163.0	169.8
Co	hcp	212.5	236.3	244.2	236.4	172.7	222.4	203.5	204.1	186.0	193.0
Ni	fcc	193.9	226.4	239.6	262.9	323.2	226.3	216.4	169.4	179.0	185.5
Cu	fcc	146.9	184.3	198.7	183.4	181.5	135.2	133.8	113.4	133.0	140.3
Zn	hcp	78.4	106.4	124.9	109.2	92.0	88.0	76.5	62.8	64.8	69.7
Y	hcp	40.7	44.4	42.1	47.0	34.5	39.9	41.5	42.5	41.0	41.7
Zr	hcp	95.5	98.3	98.7	96.9	96.3	88.0	99.0	94.4	94.9	95.9
Nb	bcc	171.1	178.9	190.6	170.4	179.2	190.6	183.7	176.7	169.0	172.0
Mo	bcc	261.3	278.2	285.3	262.9	286.8	288.4	295.7	262.8	261.0	264.7
Tc	hcp	307.6	324.1	336.5	307.2	333.3	357.2	355.4	310.2	297.0	303.1
Ru	hcp	308.2	334.8	347.6	312.5	349.5	366.3	361.9	314.1	303.0	317.7
Rh	fcc	256.4	282.8	298.5	258.8	287.6	294.0	284.7	241.2	282.0	288.7
Pd	fcc	169.4	192.1	207.9	153.3	181.4	176.0	163.3	138.8	189.0	195.4
Ag	fcc	83.3	110.2	120.9	93.6	98.3	89.9	83.6	71.2	98.8	103.8
Cd	hcp	49.6	61.1	68.0	64.1	37.9	58.1	55.3	38.9	49.8	53.8
Hf	hcp	108	112.6	115.4	116.2	114.8	112.3	115.7	111.7	108.0	109.7
Ta	bcc	195.3	205.9	212.6	201.2	210.5	217.4	205.8	193.3	191.0	193.7
W	bcc	316.2	329.8	335.7	320.1	348.2	347.0	356.4	315.9	308.0	312.3
Re	hcp	372.1	393.1	407.1	402.2	396.7	428.7	424.8	376.9	360.0	368.8
Os	hcp	402.6	426.4	449.9	427.7	482.4	460.9	460.9	396.9	418.0	424.6
Ir	fcc	347.3	367.0	391.8	339.6	396.9	397.1	392.8	328.1	358.0	365.2
Pt	fcc	250.9	272.6	290.2	250.7	273.9	278.1	275.6	225.4	277.0	284.2
Au	fcc	138.4	162.7	174.9	140.3	143.4	141.2	146.6	112.0	166.0	174.8

[a]ZPE and finite temperature corrections to experimental values adapted from Lejaeghere et al.[52]

overestimation (23%) by this functional for bulk Cr.[56] Moreover, interatomic distances of magnetic Fe, Co, and Ni are nicely described by hybrid functionals. Calculated and experimental lattice parameters are given in Table S8 of the Supporting Information.

The accuracy of all meta functionals is noticeably lower for the δ of Zn, Cd, and Re. The least accurate results, among the eight functionals considered here, are obtained by the SOGGA11 and B3LYP functionals. Upon a careful inspection of the present values and previous data,[34] one could conclude that B3LYP is even less accurate than LSDA functionals for structural data of bulk transition metals. Finally, despite satisfactory overall performance, MN12-L yields poor results for Sc and Fe.

The performance of revTPSS is not superior to that of TPSS. The reason may be that revTPSS is based on PBEsol, which was parametrized to predict better lattice constants of solid state materials, while TPSS is based on the more versatile PBE. However, for solid transition metals the performance of PBEsol is worse than that of PBE (even for interatomic distances),[34] and so is the performance of revTPSS compared to the accuracy of TPSS. In fact, revTPSS tends to be more accurate than TPSS only for heavy and late transition metals, i.e. from Zr to Cd (except Tc and Ru) and from Re to Au.

The table does show some correlation between the accuracy of the functional and the type of crystal structure. For example, M06-L and the hybrid functionals are somewhat less accurate for fcc metals with absolute errors 0.01−0.02 Å higher than average; see Tables S5−S7 in the Supporting Information for more details. At the same time, PBE0 and HSE06 are more accurate for hcp metals (MAE of only 0.014 to 0.016 Å, respectively), while M06-L, TPSS, revTPSS, and B3LYP are more accurate for bcc metals with absolute errors lower by 0.016−0.025 Å than average.

4.2. Cohesive Energies. Cohesive energies are generally harder than interatomic distances to predict correctly,[21] and Table 2 shows that many functionals are systematically biased toward overestimation or underestimation of the energies. For example, in most of the cases, the hybrid functionals considered here strongly underestimate E_{coh} by ∼1 to 1.7 eV, which renders them the least accurate functionals for this quantity (B3LYP is even less accurate than LSDA). The most accurate results come from PBE, TPSS, and N12 (MAEs of ∼0.35 eV), followed by revTPSS and SOGGA11 (MAEs of 0.52 eV).

As for interatomic distances, there are certain materials for which all meta functionals show lower accuracy. Cohesive energies of Ni, Co, and Fe are overestimated by 0.75−2 eV (except MN12-L for Co). M06-L and MN12-L also overestimate E_{coh} of Cu, Sc, and Ti. The correlation between the functional accuracy and the crystal structure is rather weak in this case, but we find that MN12-L is quite accurate for bcc metals (MAE of 0.35 eV), while PBE0 and HSE06 are particularly bad for them (MSE of ∼−1.4 eV).

4.3. Bulk Moduli. Bulk moduli are also quite hard to calculate correctly, and almost all the considered meta and hybrid functionals (except B3LYP) overestimate them, as shown in Table 3. The most accurate results are produced by PBE, followed by TPSS, while the least accurate functionals for this property are MN12-L and revTPSS.

Table 4. Statistical Analysis of Differences between the Experimental Results Extrapolated to 0 K and Corrected for Zero-Point Vibrations and the Calculated Values: Interatomic Distances (δ, in Å), Cohesive Energies (E_{coh}, in eV/atom), and Bulk Moduli (B_0, in GPa)[a]

		GGA		NGA	meta-GGA			meta-NGA	hybrid		
		PBE	SOGGA11	N12	TPSS	revTPSS	M06-L	MN12-L	PBE0	HSE06	B3LYP
δ	MSE	0.03	0.00	−0.02	0.00	−0.01	0.01	0.00	0.01	0.01	0.05
	MAE	0.04	0.05	0.05	0.04	0.04	0.05	0.05	0.03	0.03	0.06
	MAPE	1.4	1.9	1.8	1.4	1.5	1.9	2.0	1.2	1.1	2.2
	rank	3	7	6	3	5	7	9	2	**1**	10
E_{coh}	MSE	−0.04	0.40	0.12	0.21	0.50	0.46	0.40	−1.08	−0.99	−1.66
	MAE	0.34	0.52	0.36	0.35	0.52	0.49	0.64	1.08	0.99	1.66
	MAPE	10.9	11.4	8.6	10.0	11.2	10.6	13.7	24.0	21.7	37.7
	rank	4	6	**1**	2	5	3	7	9	8	10
B_0	MSE	−0.4			17.5	28.7	9.8	17.7	20.3	17.5	−8.6
	MAE	15.1			20.0	28.7	23.4	32.4	27.2	24.9	22.4
	MAPE	8.4			12.7	17.6	15.4	19.6	14.2	12.2	12.9
	rank	**1**			3	7	6	8	5	2	4
average rank	2.7	6.5	3.5	2.7	5.7	5.3	8.0	5.3	3.7	8.0	

[a]MAPE values are given in percent.

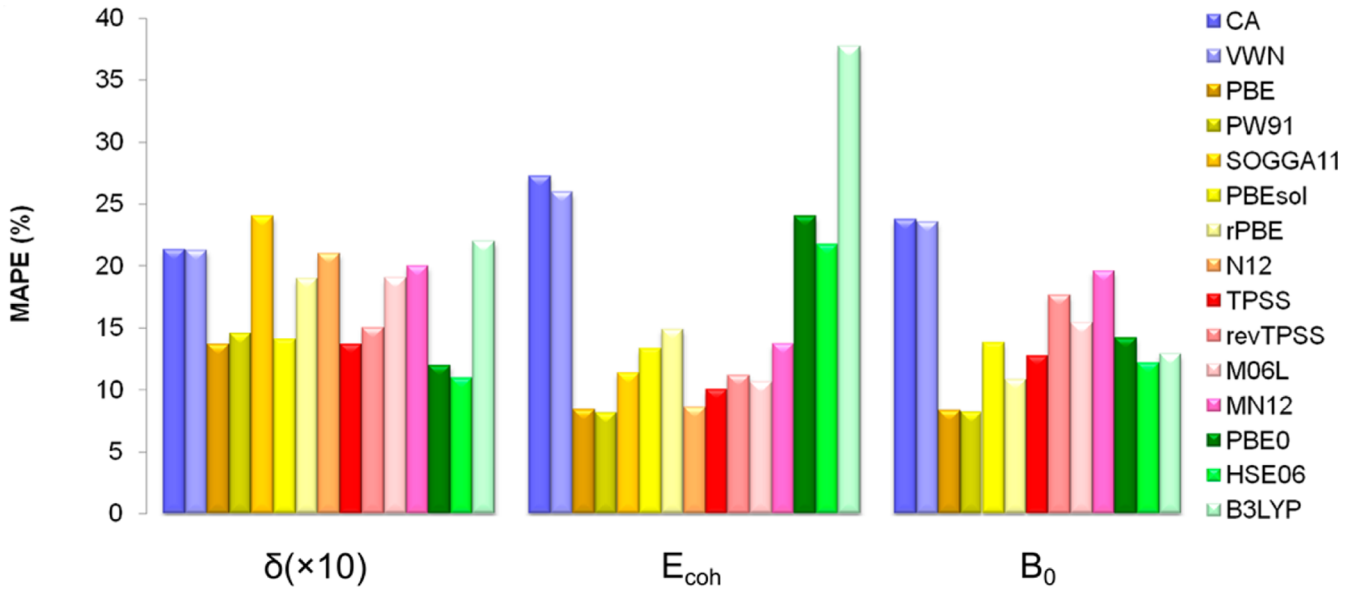

Figure 1. Mean Absolute Percentage Errors (MAPE) for the interatomic distances, δ; cohesive energies, E_{coh}; and bulk moduli, B_0, of 27 transition metals with respect to experimental values extrapolated to 0 K and adjusted to remove zero-point vibrational contributions. MAPE of δ has been multiplied by a factor of 10 for a better presentation. Data for LDA xc functionals, PBE, PW91, PBEsol, and RPBE are adapted from Janthon et al.[34]

All considered functionals significantly overestimate the bulk moduli of V, Ni, Re, and especially Cr (except B3LYP for Ni). Also, all meta functionals show lower accuracy for B_0 of Cu and Zn. The PBE and HSE06 hybrid functionals, in general, have an accuracy similar to that of meta functionals, but their performance is less satisfactory for Tc, Ru, and heavy transition metals from W to Ir.

Bulk moduli exhibit a strong correlation of functional accuracy with the crystal structure. For example, MN12-L, TPSS, revTPSS, PBE0, and HSE06 suffer a 60−70% increase in MAPE for the metals with bcc crystal structure. M06-L and B3LYP have lower accuracy for fcc metals (by 60 and 90%, respectively) but are somewhat more accurate for hcp metals (by 40 and 65%, respectively). Finally, PBE0 is 35% more accurate for B_0 of fcc metals, while HSE06 is 30% better for transition metals with hcp structure.

4.4. Overall Performance. Average discrepancies between theoretical and corrected experimental values are listed in Table 4 (for comparison with uncorrected experimental values, see Tables S2−S4, and for particular metals and properties, see Figure S1 and Tables S5−S7 in the Supporting Information). For the sake of better presentation, MAPE values are also displayed in Figure 1.

Table 4 shows the best performance is obtained for the PBE gradient approximation and for the TPSS meta functional, with HSE06, N12, M06-L, and PBE0 performing moderately well and revTPSS, B3LYP, SOGGA11, and MN12-L performing least well. TPSS is slightly more accurate than PBE for cohesive energies, while it tends to significantly overestimate bulk moduli. Both PBE and TPSS MAPE values are in line with previous calculations with a restricted set of transition metals.[55] As expected, TPSS corrects the tendency of PBE to overestimate interatomic distances by eliminating the diverging

dx.doi.org/10.1021/ct500532v | J. Chem. Theory Comput. 2014, 10, 3832−3839

exchange potential at the nuclei.[21] The use of TPSS may be favorable when molecular systems are also to be considered in the same study.[21] Nevertheless, when one is only interested in the accurate prediction of lattice parameters, hybrid functionals such as PBE0 or HSE06 may be preferred. However, HSE06 always shows a performance slightly better than that of PBE0, which may reflect the higher suitability of Hartree−Fock exchange restricted only to short range for the treatment of solid-state systems, although it may also result from cancellation of errors.

On the other hand, if one is mainly interested in accurate energetics, then the N12 gradient approximation is a good choice, especially when one considers its good performance for both cohesive energies and molecular species. The poor performance of the hybrid functionals considered here for the cohesive energies of bulk transition metals may be related to a poorer description of the gas-phase atoms used as energy references.[11] However, this does not explain the mediocre accuracy of the bulk moduli calculations with PBE0, HSE06, and B3LYP.

Although no solid-state data were used in designing M06-L, whereas solid-state data were used for designing MN12-L, it is interesting that M06-L shows better performance in the present tests. We note in passing that M06-L was found to properly describe the difficult case of CO adsorption on Pt(111), which strengthens its usefulness even in complex systems.[57] B3LYP turns out to be the least accurate hybrid functional of those studied here for transition metal solids. In most of the cases, it overestimates interatomic distances and underestimates cohesive energies, being even less accurate than LSDA. Earlier, this poor performance was explained by the LYP correlation functional not satisfying the homogeneous electron gas limit and by the inappropriateness of unscreened HF exchange for metals.[58,59]

5. CONCLUSIONS

The accuracy of selected meta and hybrid functionals for solid transition metals has been assessed by comparing calculated interatomic distances, cohesive energies, and bulk moduli to experimental values. We assess the accuracy based on the set of 27 bulk transition metals having fcc, hcp, or bcc structures. For proper comparison, the measured values were corrected for finite temperature and zero-point vibrations as in Lejaeghere et al.[52] The obtained results are also compared to those from a previous study by Janthon et al.,[34] where the performance of LSDA and GGA functionals was assessed in a very similar manner.

Table 5 presents average discrepancies between theory and experiment averaged over members of a given functional type: Gradient Approximations (GA), meta functionals, and hybrid functionals. The present results show that meta and hybrid functionals present, on average, no improvement in accuracy over gradient approximation functionals for transition metal solids. TPSS is found to be the most accurate among meta exchange-correlation functionals, but even it essentially matches the accuracy of PBE for interatomic distances and cohesive energies, while being somewhat less accurate for bulk moduli. M06-L was found to be moderately accurate as well. Given that N12, TPSS, M06-L, and MN12-L functionals are more accurate for molecular systems than PBE, one could foresee their successful application to processes involving both solid state metals and molecular species, e.g. those in surface science, heterogeneous catalysis, etc. Hybrid functionals (except B3LYP, maybe due to the uniform gas limit violation[58]) were found to be the most accurate methods for calculations of interatomic distances in bulk transition metals. However, the performance of all the hybrid functionals considered here for cohesive energies is disappointing, and their accuracy for the bulk moduli is just moderate, as expected from the known problem of HF exchange static correlation error, which is critical for the description of transition metals.

Table 5. Statistical Analysis of Differences between the Experimental Results As in Table 4 but Grouping Functionals by Type

		GA[a]	meta[b]	hybrid[c]
δ (Å)	MSE	0.00	0.00	0.03
	MAE	0.05	0.05	0.04
	MAPE	1.7	1.7	1.5
E_{coh} (eV/atom)	MSE	0.16	0.39	−1.24
	MAE	0.42	0.50	1.24
	MAPE	10.3	11.4	27.8
B_0 (GPa)	MSE	−0.4	18.4	9.7
	MAE	15.1	26.1	24.8
	MAPE	8.4	16.3	13.1

[a]Averaged over PBE, N12, and SOGGA11. [b]Averaged over TPSS, revTPSS, M06-L, and MN12-L. [c]Averaged over PBE0, HSE06, and B3LYP.

■ ASSOCIATED CONTENT

Supporting Information

Table S1 provides details of the pseudopotentials used in the calculations. Tables S2−S4 display experimental lists of interatomic distances, cohesive energies, and bulk moduli (un)corrected for ZPE and finite-temperature values, as well as differences from the two sources. Tables S5−S7 are analogous to Table 4 but considering only fcc, bcc, or hcp metals. Table S8 is analogous to Table 1 but displaying lattice constants. Figure S1 sketches the most accurate functional(s) from those studied in the description of interatomic distances, cohesive energies, and bulk moduli across the transition metals. This material is available free of charge via the Internet at http://pubs.acs.org.

■ AUTHOR INFORMATION

Corresponding Author

*E-mail: francesc.illas@ub.edu.

Notes

The authors declare no competing financial interest.

■ ACKNOWLEDGMENTS

This work was supported by Spanish *Ministerio* grants (FIS2008-02238, CTQ2012-30751) and *Generalitat de Catalunya* grants (2014SGR97 and XRQTC) and, in part, by grants from the National Science and Technology Development Agency (NSTDA Chair Professor and NANOTEC Center for the Design of Nanoscale Materials for Green Nanotechnology), the Kasetsart University Research and Development Institute (KURDI), and the Commission on Higher Education, Ministry of Education ("the National Research University Project of Thailand (NRU)" and "Postgraduate Education and Research Programs in Petroleum and Petrochemicals and Advanced Materials"). P.J. would like to thank the Office of the Higher Education Commission, Thailand for supporting him with a grant under the program Strategic Scholarships for Frontier

Research Network for the Ph.D. Program Thai Doctoral degree and the Graduate School of Kasetsart University for his research. S.M.K. thanks the *Spanish Ministerio de Educacion* for a predoctoral grant AP2009-3379. F.V. thanks the Spanish MICINN for the postdoctoral grants under the programs *Juan de la Cierva* and *Ramón y Cajal* (JCI-2010-06372 and RYC-2012-10129), and F.I. acknowledges additional support through the ICREA Academia award for excellence in research. This work was also supported in part by the Air Force Office of Scientific Research under grant number FA9550-11-1-0078.

REFERENCES

(1) Cramer, C. J.; Truhlar, D. G. *Phys. Chem. Chem. Phys.* **2009**, *11*, 10757.
(2) Perdew, J. P.; Schmidt, K. *AIP Conf. Proc.* **2001**, *577*, 1.
(3) Langreth, D. D.; Mehl, M. J. *Phys. Rev. B* **1983**, *28*, 1809.
(4) Perdew, J. P.; Wang, Y. *Phys. Rev. B* **1986**, *33*, 8800.
(5) Peverati, R.; Truhlar, D. G. *J. Chem. Theory Comput.* **2012**, *8*, 2310.
(6) Schultz, N. E.; Zhao, Y.; Truhlar, D. G. *J. Chem. Phys.* **2006**, *124*, 224105.
(7) Schultz, N. E.; Zhao, Y.; Truhlar, D. G. *J. Phys. Chem. A* **2005**, *109*, 11127.
(8) Harvey, J. N. *Annu. Rep. Prog. Chem., Sect. C* **2006**, *102*, 203.
(9) Schultz, N. E.; Zhao, Y.; Truhlar, D. G. *J. Phys. Chem. A* **2005**, *109*, 4388.
(10) Sousa, S. F.; Fernandes, P. A.; Ramos, M. J. *J. Phys. Chem. A* **2007**, *111*, 10439.
(11) Paier, J.; Marsman, M.; Hummer, K.; Kresse, G.; Gerber, I. C.; Ángyán, J. G. *J. Chem. Phys.* **2006**, *124*, 154709.
(12) (a) Polo, V.; Kraka, E.; Cremer, D. *Mol. Phys.* **2002**, *100*, 1771. (b) Grafenstein, J.; Kraka, E.; Cremer, D. *Phys. Chem. Chem. Phys.* **2004**, *6*, 1096. (c) Ellis, J. K.; Martin, R. L. *J. Chem. Theory Comput.* **2013**, *9*, 2857.
(13) (a) Jiang, W.; DeYonker, N. J.; Determann, J. J.; Wilson, A. K. *J. Phys. Chem. A* **2011**, *116*, 870. (b) Zhang, W.; Truhlar, D. G.; Tang, M. J. *J. Chem. Theory Comput.* **2013**, *9*, 3965.
(14) Perdew, J. P.; Ernzerhof, M.; Burke, K. *J. Chem. Phys.* **1996**, *105*, 9982.
(15) Marques, M. A. L.; Vidal, J.; Oliveira, M. J. T.; Reining, L.; Botti, S. *Phys. Rev. B* **2011**, *83*, 035119.
(16) Ashcroft, N. W.; Mermin, N. D. *Solid State Physics*; Saunders College Publishing: Orlando, FL, 1976; p 335.
(17) Becke, A. D. *J. Chem. Phys.* **1998**, *109*, 2092.
(18) Staroverov, V. N.; Scuseria, G. E.; Tao, J.; Perdew, J. P. *J. Chem. Phys.* **2003**, *119*, 12129.
(19) Mardirossian, N.; Parkhill, J. A.; Head-Gordon, M. *Phys. Chem. Chem. Phys.* **2011**, *13*, 19325.
(20) Peverati, R.; Truhlar, D. G. *Phys. Chem. Chem. Phys.* **2012**, *14*, 16187.
(21) Peverati, R.; Truhlar, D. G. *Philos. Trans. R. Soc., A* **2014**, *372*, 20120476.
(22) Muscat, J.; Wander, A.; Harrison, N. M. *Chem. Phys. Lett.* **2001**, *342*, 397.
(23) Tomiæ, S.; Montanari, B.; Harrison, N. M. *Phys. E* **2008**, *40*, 2125.
(24) Zhao, Y.; Truhlar, D. G. *J. Chem. Phys.* **2009**, *130*, 074103.
(25) Peverati, R.; Truhlar, D. G. *J. Chem. Phys.* **2012**, *136*, 134704.
(26) Peverati, R.; Zhao, Y.; Truhlar, D. G. *J. Phys. Chem. Lett.* **2011**, *2*, 1991.
(27) Tao, J.; Perdew, J. P.; Staroverov, V. N.; Scuseria, G. E. *Phys. Rev. Lett.* **2003**, *91*, 146401.
(28) Perdew, J. P.; Ruzsinszky, A.; Csonka, G. I.; Constantin, L. A.; Sun, J. *Phys. Rev. Lett.* **2009**, *103*, 026403.
(29) Zhao, Y.; Truhlar, D. G. *J. Chem. Phys.* **2006**, *125*, 194101.
(30) Peverati, R.; Truhlar, D. G. *Phys. Chem. Chem. Phys.* **2012**, *14*, 13171.
(31) Adamo, C.; Barone, V. *J. Chem. Phys.* **1999**, *110*, 6158.
(32) Becke, A. D. *J. Chem. Phys.* **1993**, *98*, 5648.
(33) Krukau, A. V.; Vydrov, O. A.; Izmaylov, A. F.; Scuseria, G. E. *J. Chem. Phys.* **2006**, *125*, 224106.
(34) Janthon, P.; Kozlov, S. M.; Viñes, F.; Limtrakul, J.; Illas, F. *J. Chem. Theory Comput.* **2013**, *9*, 1631.
(35) Perdew, J. P.; Zunger, A. *Phys. Rev. B* **1981**, *23*, 5048.
(36) Ceperley, D. M.; Alder, B. J. *Phys. Rev. Lett.* **1980**, *45*, 566.
(37) Vosko, S. H.; Wilk, L.; Nusair, M. *Can. J. Phys.* **1980**, *58*, 1200.
(38) Perdew, J. P.; Burke, K.; Ernzerhof, M. *Phys. Rev. Lett.* **1996**, *77*, 3865.
(39) Perdew, J. P.; Ruzsinszky, A.; Csonka, G. I.; Vydrov, O. A.; Scuseria, G. E.; Constantin, L. A.; Zhou, X.; Burke, K. *Phys. Rev. Lett.* **2008**, *100*, 136406.
(40) Hammer, B.; Hansen, L. B.; Nørskov, J. K. *Phys. Rev. B* **1999**, *59*, 7413.
(41) Perdew, J. P.; Wang, Y. *Phys. Rev. B* **1992**, *45*, 13244.
(42) Kresse, G.; Furthmüller, J. *Phys. Rev. B* **1996**, *54*, 11169.
(43) Blöchl, P. E. *Phys. Rev. B* **1994**, *50*, 17953.
(44) Monkhorst, H. J.; Pack, J. D. *Phys. Rev. B* **1976**, *13*, 5188.
(45) Grabowski, B.; Hickel, T.; Neugebauer, J. *Phys. Rev. B* **2007**, *76*, 024309.
(46) Billas, I. M. L.; Châtelain, A.; de Heer, W. A. *Science* **1994**, *265*, 1682.
(47) Hafner, R.; Spišák, D.; Lorenz, R.; Hafner, J. *Phys. Rev. B* **2002**, *65*, 184432.
(48) Blöchl, P. E.; Jepsen, O.; Andersen, O. K. *Phys. Rev. B* **1994**, *49*, 16223.
(49) Murnaghan, F. D. *Proc. Natl. Acad. Sci. U. S. A.* **1944**, *30*, 244.
(50) Gražulis, S.; Chateigner, D.; Downs, R. T.; Yokochi, A. T.; Quiros, M.; Lutterotti, L.; Manakova, E.; Butkus, J.; Moeck, P.; Le Bail, A. J. *Appl. Crystallogr.* **2009**, *42*, 726.
(51) Young, D. A. *Phase Diagrams of the Elements*; University of California Press: Berkeley, CA, 1991; p 273.
(52) Lejaeghere, K.; Van Speybroeck, V.; Van Oost, G.; Cottenier, S. *Crit. Rev. Solid State Mater. Sci.* **2014**, *39*, 1.
(53) Kittel, C. *Introduction to Solid State Physics*, 8th ed.; John Wiley & Sons, Inc.: New York, 2005; p 20.
(54) Villars, P.; Daams, J. *J. Alloys Compd.* **1993**, *197*, 177.
(55) Haas, P.; Tran, F.; Blaha, P. *Phys. Rev. B* **2009**, *79*, 085104.
(56) Chevrier, V. L.; Ong, S. P.; Armiento, R.; Chan, M. K. Y.; Ceder, G. *Phys. Rev. B* **2010**, *82*, 075122.
(57) Luo, S.; Zhao, Y.; Truhlar, D. G. *J. Phys. Chem. Lett.* **2012**, *3*, 2975.
(58) Kurth, S.; Perdew, J. P.; Blaha, P. *Int. J. Quantum Chem.* **1999**, *75*, 889.
(59) Paier, J.; Marsman, M.; Kresse, G. *J. Chem. Phys.* **2007**, *127*, 024103.